

Small-Signal Modulation and Analysis of Monolithic 1.3 μm InAs/GaAs Quantum Dot Lasers on Silicon

C. Hantschmann⁽¹⁾, P. P. Vasil'ev^(1,3), S. Chen⁽²⁾, M. Liao⁽²⁾, A. J. Seeds⁽²⁾, H. Liu⁽²⁾, R. V. Pentyl⁽¹⁾, I. H. White⁽¹⁾

⁽¹⁾ Centre for Photonic Systems, Department of Engineering, University of Cambridge, 9 JJ Thomson Avenue, Cambridge CB3 0FA, UK, cb893@cam.ac.uk

⁽²⁾ Department of Electronic and Electrical Engineering, University College London, Torrington Place, London WC1E 7JE, UK

⁽³⁾ Also associated with the PN Lebedev Physical Institute, 53 Leninsky Prospect, Moscow 119991, Russia

Abstract *The first small-signal modulation experiments with monolithic single transverse mode InAs/GaAs lasers on Si demonstrate a 3dB bandwidth of 1.6 GHz. By fitting the modulation response curves, we extract high-speed laser parameters allowing an insight into the intrinsic laser dynamics.*

Introduction

The first demonstration of 1.3 μm InAs/GaAs quantum dot (QD) lasers monolithically grown on silicon (Si) able to operate continuous-wave (cw) at room temperature was a breakthrough in the field of semiconductor lasers¹. The true potential of monolithic QD lasers on Si substrates, however, goes far beyond photonic integrated circuits, and spans from high-power lasers with good thermal dissipation to low-cost Datacom lasers. So far, numerous studies on the optimisation of the cw performance of these novel lasers have been published, but the dynamic properties are largely unexplored^{2,3}. In particular, it is not yet known if the performance of Si-based InAs/GaAs QD lasers will be inherently affected by the strong lattice mismatch between the substrate and the laser structure, or if in fact values similar to those demonstrated with QD lasers on GaAs substrates could be achieved if a rigorous design optimisation for high-speed performance is performed. In this paper, we report the first results of small-signal and large-signal modulation of monolithic cw 1.3 μm narrow ridge-waveguide III-V QD lasers on Si with a 3dB frequency of 1.6 GHz and an open eye at 1.5 Gb/s. A dynamic analysis suggests that strong damping, reflected in a K -factor of 3.7 ns, limits the modulation bandwidth. This could be improved by a short cavity design with an increased number of active layers and a higher dot density.

Theory

QD lasers are commonly modelled by multi-level rate equation systems, which describe the carrier dynamics within the discrete energy levels of QDs embedded in a wetting layer with a

continuum of energy states⁴. Nevertheless, the small-signal frequency response of a QD laser is often analysed using a three-pole transfer function

$$|H(f)|^2 = \frac{f_R^4}{(f_R^2 - f^2)^2 + \left(\frac{\gamma f}{2\pi}\right)^2} \cdot \frac{1}{1 + \left(\frac{f}{f_p}\right)^2} \quad (1)$$

derived from the one-level rate equation⁵, as it allows a straightforward analysis of experimental data using the resonance frequency f_R , the damping γ , and the frequency f_p given by parasitic circuit elements⁶.

A few key parameters can be used for understanding and comparing the observed results. The D -factor links the resonance frequency to the current above threshold as

$$f_R = D \cdot \sqrt{I - I_{th}} \quad (2)$$

and is, thus, a means of quantifying how fast the resonance frequency increases with current⁶. By replacing f_R with the 3dB frequency, f_{3dB} , this rate is similarly expressed through the modulation current efficiency $MCEF$ instead of the D -factor. Furthermore, the relationship between the damping and the resonance frequency,

$$\gamma = K f_R^2 + \gamma_0, \quad (3)$$

allows calculation of the damping offset, γ_0 , which depends on the inverse effective carrier lifetime in the QD laser, and K -factor. The latter is an especially important parameter in determining the high-speed potential of a laser, as the maximum achievable 3dB bandwidth depends inversely on it⁵.

Laser structure and static performance

The InAs/GaAs QD laser studied here is grown on a Si substrate with a 4° offcut. To reduce the

density of threading dislocations propagating up into the active region from the GaAs/Si interface, various buffer layers are grown first. A detailed description of the growth process and the epitaxial structure can be found in ⁷. The active region of the laser is sandwiched between a *p*- and an *n*-doped cladding layer and consists of five stacked InAs/InGaAs/GaAs dot-in-a-well layers with an approximate QD density of $3 \times 10^{10} \text{ cm}^{-2}$. A highly *p*-doped layer completes the QD laser to allow a good electrical contact. Narrow ridge-waveguide lasers are fabricated using standard semiconductor device fabrication techniques. The laser has dimensions of $2.2 \mu\text{m} \times 2.5 \text{ mm}$ with a high reflectivity coating on the rear facet and an as-cleaved front facet. Finally, the lasers are mounted on a copper heatsink for improved thermal dissipation.

All measurements are performed under cw current injection at room temperature with the heatsink temperature set to 15 °C. Under these conditions, the QD laser shows a laser threshold of 20 mA with a slope of about 0.09 mW/mA. The lasing spectrum is centred around 1310 nm in a single transverse mode.

Small-signal and large-signal modulation

A vector network analyser (VNA) is used to investigate the dynamic response of the QD laser. A -5 dBm RF signal that is swept over a frequency range from 50 MHz to 6 GHz is superimposed to DC drive currents between about 25 mA and 40 mA. The modulated light is collected with a singlemode fibre connected to the VNA, where the small-signal modulation response is computed. Fig. 1(a) shows the smoothed and normalised modulation response curves together with the three-pole transfer function fits. The 3dB bandwidth increases with current, reaching a maximum modulation bandwidth of 1.6 GHz at 40.0 mA.

Optical eye patterns are measured by modulating the laser with a non-return-to-zero (NRZ) signal from a random bit pattern generator. The respective eye diagrams being displayed on an oscilloscope can be seen in Fig. 1(b). Clear eyes are recorded at 1.0 Gb/s and at 1.5 Gb/s. At 2.0 Gb/s, the eye is closed.

Analysis and Discussion

The modulation response curves shown in Fig. 1(a) are analysed by the fit as given in Eq. (1). A very good agreement between the fit and the data is found. Fig. 2(a) displays f_R and f_{3dB} plotted against the current above threshold. A linear fit gives a *D*-factor of about 0.3 GHz/mA^{1/2}, which is comparable to the *D*-factors of about 0.4 to 0.5 GHz/mA^{1/2} which have been obtained

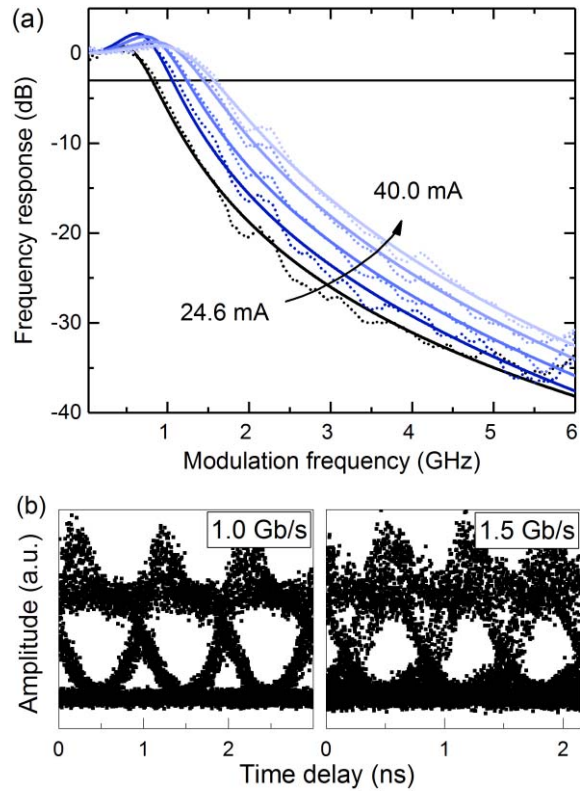


Fig. 1: (a) Small-signal modulation response curves of the QD laser on Si recorded at 24.6 mA, 27.5 mA, 30.0 mA, 35.5 mA, and 40.0 mA. (b) NRZ modulation optical eye patterns at data rates of 1.0 Gb/s (left) and 1.5 Gb/s (right) with the laser biased close to the threshold.

during the earlier work on InAs QD lasers grown on GaAs⁸. At small currents, a modulation current efficiency of approximately 0.4 GHz/mA^{1/2} is calculated, reflecting that the modulation bandwidth is about 50 % larger than the resonance frequency at low damping, whereas the sublinear trend towards higher currents indicates that strong damping begins to limit the modulation bandwidth^{4,5}.

Fig. 2(b) shows the damping plotted against the squared resonance frequencies. Omitting the first data point, a clear linear dependence can be seen, which gives a large *K*-factor of 3.7 ns, while the damping offset γ_0 is 2.0 GHz, corresponding to an effective carrier lifetime of 0.5 ns. This reveals that the measured small-signal curves are strongly damping limited, which is most likely a result of a long photon lifetime along with reduced differential gain, or high gain compression⁵.

Conventional GaAs-based QD lasers in general have inferior high-speed properties compared with quantum well lasers, having demonstrated 3dB bandwidths ranging from smaller than 4 GHz⁹ to 12 GHz¹⁰ and an exceptionally fast value of 16 GHz¹¹. Most of these devices have short cavities of about

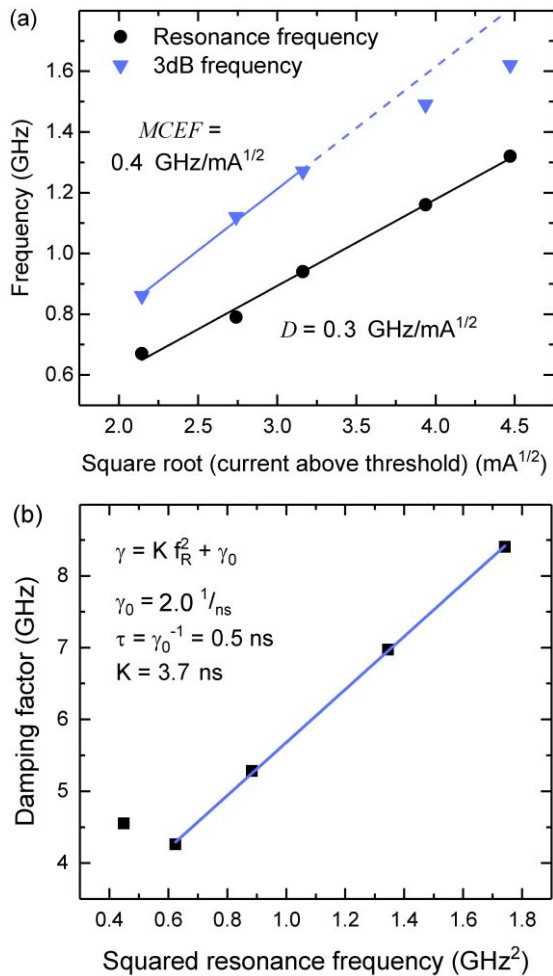


Fig. 2: (a) Resonance and 3dB frequencies versus the square root of the current above threshold. The two linear fits give the D -factor and the modulation current efficiency, respectively (b) Damping versus the squared resonance frequency. The linear fit according allows to extract the K -factor from the fit's slope and the damping offset from the y -axis intercept.

400 – 1000 μm^{8-11} and include up to ten QD layers for high gain^{6,11}, whereas the geometry and the epitaxial structure of the Si-based QD laser are not yet designed for high-speed operation. Analytical modelling predicts that 3.5 GHz and 5.0 GHz would be feasible by reducing the cavity lengths to 1 mm and 500 μm , respectively, and doubling the number of QD layers in the active region. Introducing a p -doped active region should further speed up the devices by providing higher differential gain⁵.

Conclusions

We have presented the first small-signal and large-signal modulation results of monolithic cw 1.3 μm narrow ridge-waveguide InAs/GaAs QD lasers grown Si substrate, demonstrating a maximum 3dB frequency of 1.6 GHz and an open eye at 1.5 Gb/s. From fitting the curves with the three-pole transfer function, a D -factor of

0.3 GHz/mA^{1/2}, a modulation current efficiency of 0.4 GHz/mA^{1/2}, an effective carrier lifetime of 0.5 ns and a K -factor of 3.7 ns have been derived. Given that the device has not been optimised for high speed, modelling suggests that modulation bandwidths of 5 GHz could be achieved by an optimised QD laser design readily on the basis of the current growth process by scaling the number of QD layers and the cavity length. Further improvements are likely using additional approaches such as a p -doped active region.

Acknowledgements

This work is supported by UK EPSRC at the University of Cambridge and at University College London (UCL Grant No. EP/J0129041/1, EP/J012815/1). C. Hantschmann wishes to thank Qualcomm Inc. for PhD funding. S. Chen's research fellowship is funded by the Royal Academy of Engineering (Reference No. RF201617/16/28).

References

- [1] A. Lee et al., "Continuous-Wave InAs/GaAs Quantum-Dot Laser Diodes Monolithically Grown on Si Substrate with Low Threshold Current Densities," *Opt. Express*, Vol. **20**, no. 20, p. 22181 (2012)
- [2] A. Y. Liu et al., "Reflection Sensitivity of 1.3 μm Quantum Dot Lasers Epitaxially Grown on Silicon," *Opt. Express*, Vol. **25**, no. 9, p. 9535 (2017).
- [3] Z. Mi et al., "High Performance Self-Organized InGaAs Quantum Dot Lasers on Silicon," *J. Vac. Sci. Technol. B*, Vol. **24**, no. 3, p. 1519 (2006).
- [4] A. Fiore and A. Markus, "Differential Gain and Gain Compression in Quantum-Dot Lasers," *IEEE J. Quantum Electron.*, Vol. **43**, no. 4, p. 287 (2007).
- [5] L. A. Coldren and S. W. Corzine, *Diode Lasers and Photonic Integrated Circuits*, John Wiley & Sons (1995).
- [6] D. Arsenijević and D. Bimberg, "Quantum-Dot Lasers for 35 Gbit/s Pulse-Amplitude Modulation and 160 Gbit/s Differential Quadrature Phase-Shift Keying," *Proc. of SPIE*, Vol. **9592**, p. 95920S-1 (2016).
- [7] S. Chen et al., "Electrically Pumped Continuous-Wave III-V Quantum Dot Lasers on Silicon," *Nat. Photonics*, Vol. **10**, no. 5, p. 307 (2016).
- [8] R. Krebs et al., "High Frequency Characteristics of InAs/GaInAs Quantum Dot Distributed Feedback Lasers Emitting at 1.3 μm ," *Electron. Lett.*, Vol. **37**, no. 20, p. 1223 (2001).
- [9] K. T. Tan et al., "High Bit Rate and Elevated Temperature Data Transmission Using InGaAs Quantum-Dot Lasers," *IEEE Photon. Technol. Lett.*, Vol. **16**, no. 5, p. 1415 (2004).
- [10] S. M. Kim et al., "High-Frequency Modulation Characteristics of 1.3- μm InGaAs Quantum Dot Lasers," *IEEE Photon. Technol. Lett.*, Vol. **16**, no. 2, p. 377 (2004).
- [11] M. Ishida et al., "Temperature-Stable 25-Gbps Direct-Modulation in 1.3- μm InAs/GaAs Quantum Dot Lasers," *CLEO, CM112*, San Jose (2012).